Molecular and Cellular Neuroscience 131 (2024) 103977

Contents lists available at ScienceDirect

Molecular and Cellular Neuroscience

journal homepage: www.elsevier.com/locate/ymcne

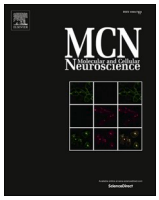

Inhibition of phosphodiesterase 10A mitigates neuronal injury by modulating apoptotic pathways in cold-induced traumatic brain injury

Mustafa C. Beker [a,b,*], Mehmet O. Altintas [c], Enes Dogan [b], Cigdem Bayraktaroglu [b], Buse Balaban [b,d], Aysenur Ozpinar [b], Nursena Sengun [a], Serdar Altunay [b], Ertugrul Kilic [a,b]

[a] Department of Physiology, School of Medicine, Istanbul Medeniyet University, Istanbul, Türkiye
[b] Regenerative and Restorative Medical Research Center (REMER), Research Institute for Health Sciences and Technologies (SABITA), Istanbul Medipol University, Istanbul, Türkiye
[c] Department of Physiology, School of Medicine, Ankara Medipol University, Ankara, Türkiye
[d] Department of Medical Biology, Institute of Health Sciences, University of Health Sciences Turkey, Istanbul, Türkiye

ARTICLE INFO

Keywords:
cAMP
Cold injury
PDE10A
Phosphodiesterase-10A
TAK-063
Traumatic brain injury

ABSTRACT

Brain injury develops from a complex series of pathophysiological phases, resulting in acute necrotic or delayed apoptotic cell death after traumatic brain injury (TBI). Inhibition of apoptotic cell death is critical for the treatment of acute neurodegenerative disorders, such as TBI. Here, we investigated the role of phosphodiesterase 10A (PDE10A) in the development of neuronal injury, particularly in apoptotic cell death. Using the PDE10A inhibitor TAK-063, we found that PDE10A inhibition is associated with decreased brain injury, brain swelling, and blood brain barrier disruption 48 h after cold-induced TBI. Furthermore, a particularly notable result was observed with 3 mg/kg TAK-063, which reduced disseminated neuronal injury. Protein abundance analysis revealed that PDE10A inhibition activates survival kinases AKT and ERK-1/-2, which were associated with the decreased activation of MMP-9 and PTEN. Additionally, iNOS and nNOS levels significantly reduced in the TAK-063 group, playing roles in inflammation and apoptosis. A planar surface immunoassay was performed for in-depth analyses of the apoptotic signaling pathways. We observed that inhibition of PDE10A resulted in the decreased expression of TNFRSF1A, TNFRSF10B, and TNFRSF6 receptors, particularly inducing apoptotic cell death. Moreover, these findings correlated with reduced levels of pro-apoptotic proteins, including PTEN, p27, Cytochrome-c, cleaved Caspase-3, Bad, and p53. Interestingly, TAK-063 treatment reduced levels of anti-apoptotic proteins or enzymes, including XIAP, Claspin, and HIF1α, without affecting Bcl-x, MCL-1, SMAC, HO-1, HO-2, HSP27, HSP60, and HSP70. The findings suggest that PDE10A regulates cellular signaling predominantly pro-apoptotic pathways, and inhibition of this protein is a promising approach for the treatment of acute brain injury.

Abbreviations: cAMP, Adenosine 3′,5′-Cyclic Monophosphate; PKA, Activating Protein Kinase A; BCL-2, B-Cell Lymphoma-2; BAD, BCL2-Associated Agonist Of Cell Death; BBB, Blood-Brain Barrier; BDNF, Brain-Derived Neurotrophic Factor; CREB, cAMP Response Element-Binding Protein; CNS, Central Nervous System; P27/Kip1, Cyclin-Dependent Kinase Inhibitor P27; DMSO, Dimethyl Sulfoxide; DAPI, 4′,6-Diamidino-2-Phenylindole; Fas/TNFRSF6/CD95, Fas Receptor; cGMP, Guanosine 3′,5′-Cyclic Monophosphate; HSP60, Heat Shock 60 kDa Protein; HSP70/HSPA1A, Heat Shock 70 kDa Protein; HO-1/HMOX1/HSP32, Heme Oxygenase-1; HO-2/HMOX2, Heme Oxygenase-2; HD, Huntington's Disease; HIF-1α, Hypoxia-Inducible Factor 1 Alpha; iNOS, Inducible Nitric Oxide Synthase; MMP9, Matrix Metalloproteinase-9; MCL-1, Myeloid Cell Leukemia-1; nNOS, Neuronal Nitric Oxide Synthase; NF-κB, Nuclear Factor Kappa B; PFA, Paraformaldehyde; PD, Parkinson's Disease; PBS, Phosphate-Buffered Saline; PDE10A, Phosphodiesterase 10A; PDEs, Phosphodiesterases; PKG, Protein Kinase G; ROI, Regions Of Interest; SMAC/Diablo, Second Mitochondria-Derived Activator Of Caspases; TUNEL, Terminal Deoxynucleotidyl Transferase dUTP Nick End Labeling; TBI, Traumatic Brain Injury; TNFRSF10B, Tumor Necrosis Factor Receptor Superfamily Member 10B; TNFR2, Tumor Necrosis Factor-Alpha Receptor-2; TNF RI/TNFRSF1A, Tumor Necrosis Factor Receptor I; P53, Tumor Protein P53; XIAP, X-Linked Inhibitor Of Apoptosis Protein.

* Corresponding author at: Department of Physiology, Istanbul Medeniyet University, Ünalan Mahallesi Ünalan Sokak, D100 Karayolu, Yanyol, 34700 Üsküdar/İstanbul, Türkiye.

E-mail address: mustafa.beker@medeniyet.edu.tr (M.C. Beker).

https://doi.org/10.1016/j.mcn.2024.103977
Received 30 August 2024; Received in revised form 7 October 2024; Accepted 14 October 2024
Available online 20 October 2024

1. Introduction

Phosphodiesterases (PDEs) play an essential role in the inactivation of adenosine 3′,5′-cyclic monophosphate (cAMP) and guanosine 3′,5′-cyclic monophosphate (cGMP), which are crucial second messengers that actively participate in a wide range of physiological and pathophysiological processes within the central nervous system (CNS), such as neuronal development, neuronal injury, neuroplasticity, and DNA fragmentation (Delhaye and Bardoni, 2021; Titus et al., 2015). It is well known that 21 genes responsible for encoding PDEs formed 11 unique PDE families and splice variants (PDE1-PDE11) (Lugnier, 2022). Among PDEs, Phosphodiesterase 10A (PDE10A) has recently gained significant attention due to its distinct distribution within the CNS.

PDE10A is an enzyme exhibiting dual-substrate specificity, capable of hydrolyzing cAMP and cGMP. Its presence is particularly prominent in the basal ganglia/striatum, yet it is also found distributed in the cortex and various other regions of the brain (Argyrousi et al., 2020). Inhibition of PDE10A results in increased levels of cAMP and cGMP, activating protein kinase A (PKA) and cGMP/protein kinase G (PKG). This activation, in turn, initiates an essential intracellular signal transduction pathway. Recent studies also reveal that cAMP has a dual role in the cell death processes in a tissue-dependent manner (Insel et al., 2012). It was shown that agents elevating cAMP, such as forskolin, inhibit the activation of apoptosis signaling and promote the anti-apoptotic pathway in macrophages (Misra and Pizzo, 2005).

Recent research has highlighted the significance of PDE10A as a promising therapeutic target in the management of neurodegenerative conditions, including ischemic stroke, Huntington's disease (HD), and Parkinson's disease (PD) (Beker et al., 2022a; Beker et al., 2022b; Birjandi et al., 2021; Garcia et al., 2014; Ito et al., 2018; Niccolini et al., 2015; Padovan-Neto and West, 2017). Previously, we demonstrated that the inhibition of PDE10A reduces brain infarct size, mitigates widespread neuronal injury, and improves cerebral microcirculation, neurogenesis, angiogenesis, functional recovery, and neuroplasticity in a mouse model of ischemic stroke (Beker et al., 2022a; Beker et al., 2022b). Furthermore, pharmacological inactivation of PDE10A has been shown to activate neurotrophic factors, including brain-derived neurotrophic factor (BDNF), ciliary neurotrophic factor, fibroblast growth factor, and mesencephalic astrocyte-derived neurotrophic factor (Beker et al., 2022b; Birjandi et al., 2021). Giampà et al. demonstrated that PDE10A inhibition increased phosphorylated cAMP response element-binding protein (CREB) and BDNF expression in R6/2 mice, a model of HD, thereby reducing striatal and cortical pathology (Giampa et al., 2010). Additionally, PDE10A inhibition mediated by MP10 ameliorated behavioral impairments and reversed the loss of dopaminergic neurons in the brains of mice induced with 1-methyl-4-phenyl-1,2,3,6-tetrahydropyridine, a model of PD (Kim et al., 2021). Moreover, a recent study demonstrated that PDE10A inhibition exerts protective effects following TBI by reducing neuroinflammation and inhibiting apoptosis, partially through the cAMP/PKA/NLRP3 pathway. This inhibition also improved learning and memory functions in rats with TBI (Huang et al., 2022). In another study, PDE10A protein abundance was increased in the cortex but decreased in the hippocampus acutely after TBI (Wilson et al., 2016).

Although the positive impact of PDE10A inhibition on various neurodegenerative disorders is known, its effect on the pathophysiology of TBI, particularly on apoptotic cell death, remains largely unknown. The present study aims to investigate the neuroprotective role of PDE10A inhibition after TBI. For the induction of TBI, animals were submitted to cold-induced traumatic brain injury, a commonly used animal model that shares essential similarities with cerebral ischemia in pathophysiological cascades (Hermann et al., 2001; Kelestemur et al., 2016). To pharmacologically inhibit PDE10A, we utilized TAK-063, a potent, orally bioavailable, and particular inhibitor of PDE10A (Suzuki and Kimura, 2018). Immediately after TBI, animals were treated with a low dose (0.3 mg/kg) or a high dose (3 mg/kg) of TAK-063 per oral. We initially evaluated brain infarct volume, brain swelling, and blood-brain barrier (BBB) permeability which was evaluated by Evans blue staining. To understand the underlying molecular mechanisms, we analyzed the protein abundances of survival kinases p-AKT and p-ERK-1/2, p-PTEN, MMP9, iNOS, and nNOS by Western blotting. For in-depth analysis of apoptotic signaling pathways, we performed a planar surface immunoassay to evaluate the expression levels of pro- and anti-apoptotic proteins.

2. Material and methods

2.1. Animals and cold-induced traumatic brain injury

Experiments have been conducted under the ethics standards of the EU Guidelines on the Care and Use of Laboratory Animals (Directive 2010/63/EU) in agreement with local guidelines and legislation. The study has been approved by local government authorities (Istanbul Medipol University, Animal Research Ethics Committee; reference number: 03/02/2021-10). We maintained all animals in a controlled environment with a consistent 12-hour light/dark cycle, providing them unrestricted access to food and water.

The TBI procedure was conducted following a modified version of the cold injury-induced trauma model described previously (Kelestemur et al., 2016). In brief, 33 male Balb/C mice, aged 8–12 weeks, were anesthetized using 1 % isoflurane (30 % O_2, with the remaining balance as N_2O) and placed on a stereotaxic device (WPI Instruments, USA). The rectal temperature was controlled between 36.5 and 37.0 °C throughout the experimental procedures using a homoeothermic blanket. Brain injury was induced by applying a liquid nitrogen-cooled copper probe with a tip diameter of 2.0 mm (positioned at Bregma 2.0 mm posterior and 1.5 mm lateral), directly placed on the skull for 60 s, and removed (Ciftci et al., 2020; Kelestemur et al., 2016; Keskin et al., 2017). Then, wounds were closed with sutures before anesthesia was discontinued.

To inhibit PDE10A, we used TAK-063 (510331, MedKoo Biosciences, USA), which was dissolved in a 1 % (*v*/v) solution of dimethyl sulfoxide (DMSO) in tap water. After animal surgery, mice were randomly divided into three groups: vehicle group (100 µl of water containing 1 % DMSO), 0.3 mg/kg TAK-063 (TAK-063 dissolved in 100 µl of water containing 1 % DMSO), and 3 mg/kg TAK-063 group (TAK-063 dissolved in 100 µl of water containing 1 % DMSO) ($n = 11$/group). Vehicle, or TAK-063, was administered just after TBI per oral. Forty-eight hours after trauma, $n = 7$ per group animals were deeply anesthetized with 4 % isoflurane (30 % O_2, remainder N_2O) and decapitated. Brains were removed, frozen on dry ice, and cut on a cryostat (CM1950, Leica, Germany) into 18 µm sections used for infarct volume, brain swelling, neuronal survival, and DNA fragmentation analysis. Further tissue was collected from the ipsilesional hemisphere of all animals for Western blot and planar surface immunoassay analysis (Kilic et al., 2017). In addition, 48 h after cold-induced TBI, Evans blue was applied to 4 mice per group for BBB integration, and then the mice were sacrificed.

2.2. Determination of infarct volume and brain swelling

To assess brain infarct volume and cytotoxic edema, coronal brain sections ($n = 7$ mice* 3 brain sections) were collected at equidistant intervals of 1 mm, stained with Cresyl violet (C5042; Sigma-Aldrich, USA), following a previously published protocol (Beker et al., 2015). The border between injured and non-injured tissues was delineated within the sections using image analysis software (Image J; National Institute of Health, USA). The infarct area was quantified by subtracting the area of the non-infarcted ipsilesional hemisphere from that of the contralesional side. Infarct volume was calculated by the integration of these areas. Brain swelling was determined as the volume difference between the injured and the non-injured hemisphere and expressed in cubic millimeters (mm^3) (Yelkenci et al., 2024).

2.3. Analysis of neuronal survival

Neuronal survival was assessed following a previously described protocol (Beker et al., 2019). Coronal brain sections (n = 7 mice* 2 different brain sections) were fixed using 4 % paraformaldehyde (PFA) in 0.1 M phosphate-buffered saline (PBS), washed, and then immersed in 0.1 M PBS with 0.3 % Triton X-100 (PBS-T) and 10 % normal goat serum for 1 h. Subsequently, the sections were incubated overnight at 4 °C with Cy3-conjugated monoclonal mouse anti-NeuN (MAB377C3; Merck, USA). The following day, the sections were exposed to 4′,6-diamidino-2-phenylindole (DAPI; 422801, BioLegend, USA). Imaging and analysis were performed using a Zeiss LSM 800 confocal laser scanning microscope (Carl Zeiss, Germany). Six distinct regions of interest (ROI) within the cortex, each measuring 62,500 μm^2, were evaluated. The mean numbers of NeuN-positive cells were quantified in both the injured and non-injured cortex. To determine the percentage of surviving neurons in the ipsilesional tissue, the results from the injured cortex were divided by the results from the non-injured cortex and multiplied by 100.

2.4. Analysis of apoptotic cell death

Brain sections (n = 7 mice* 2 different brain sections) were fixed with 4 % PFA/0.1 M PBS to evaluate the DNA fragmentation. Then, sections were labeled using a TUNEL assay kit (In Situ Cell Death Detection Kit; Roche, Switzerland) according to the previously described protocol (Beker et al., 2015). Sections were counterstained with DAPI. Stainings were analyzed using a Zeiss LSM 800 confocal laser scanning microscope (Carl Zeiss, Jena, Germany). We quantified the number of TUNEL-positive cells in six adjacent ROI within the injured cortex at the level of hippocampus, with each ROI measuring 62,500 μm^2.

2.5. Analysis of blood-brain barrier (BBB) integrity

Evans blue staining was performed to examine the BBB permeability after cold-induced TBI. Evans Blue (E2129-10G; Sigma-Aldrich) was prepared at 2 % (w/v) in normal saline. The dye solution (3 ml/kg) was administered through the tail vein toward blood flow. One hour after injection, the animals (n = 4 per group) were sacrificed by decapitation. The whole brain was removed and cut coronally into 2-mm slices using a brain matrix, with cutting sites corresponding to −2 mm AP distance from the bregma. Sections (n = 4 mice* 2 images) were analyzed using an image analysis system (Image J).

2.6. cAMP quantification using ELISA

To assess cAMP levels in cortical tissues following TBI, samples were collected from the injured cortex region. cAMP quantification was performed using the Cyclic AMP XP® Assay Kit (4339, Cell Signaling Technologies), according to the manufacturer's instructions. Briefly, tissue homogenates were prepared, and cAMP levels were measured via enzyme-linked immunosorbent assay (ELISA). Absorbance was read at 450 nm using a microplate reader (MultiSkan™ GO, ThermoFisher Scientific), and cAMP concentrations were calculated from a standard curve generated with known cAMP concentrations. Data were normalized to protein content in each sample (Elibol et al., 2020).

2.7. Western blot

For the Western blot analysis, tissue samples from the injured cortex within the same experimental group were pooled. These combined samples (n = 7 per group) were then homogenized, sonicated, and treated with a protease/phosphatase inhibitor cocktail (5872, Cell Signaling Technology) (Beker et al., 2020). Total protein content was evaluated using a Qubit 3.0 Fluorometer (Q33216, Invitrogen, Life Technologies Corporation, USA) following the manufacturer's instructions. Equivalent amounts of protein (20 μg) were separated through gel electrophoresis using a 4–20 % Mini-PROTEAN TGX gel (4561096, Biorad Life Sciences Research) and subsequently transferred to a PVDF membrane utilizing the Trans-Blot Turbo Transfer System (1704155, Biorad Life Sciences Research). Following that, the membranes underwent a blocking step with a 5 % nonfat milk solution in 50 mM Tris-buffered saline (TBS) containing 0.1 % Tween (TBS-T) for 1 h at room temperature. They were then rinsed in 50 mM TBS-T and subsequently incubated overnight with the following antibodies: monoclonal mouse PDE10 (sc-515023; Santa Cruz Biotechnology), polyclonal rabbit anti-phospho-Akt (9275, Cell Signaling Technology), polyclonal rabbit anti-Akt (9272; Cell Signaling Technology), polyclonal rabbit anti-phospho-PTEN (9551; Cell Signaling Technology), polyclonal rabbit anti-PTEN (9552; Cell Signaling Technology), monoclonal rabbit anti-phospho-p44/42 MAPK (Erk1/2) (4370; Cell Signaling Technology), polyclonal rabbit anti-p44/42 MAPK (Erk1/2) (9102; Cell Signaling Technology), polyclonal rabbit anti-MMP-9 (Ab38898, Abcam, UK), monoclonal mouse iNOS (sc-7271, Santa Cruz Biotechnology), and monoclonal mouse nNOS (sc-5302, Santa Cruz Biotechnology). The following day, the membranes were washed with 50 mM TBS-T and exposed to horseradish peroxidase-conjugated goat-anti-rabbit (sc-2004, Santa Cruz Biotechnology) or goat anti-mouse (sc-2005, Santa Cruz Biotechnology) antibodies, both diluted at 1:2500, for 1 h at room temperature. This blotting procedure was repeated at least three times for consistency. A polyclonal rabbit anti-β-actin antibody (4967, Cell Signaling Technology) was employed to verify equal protein loading. Blots were developed using the Clarity Western ECL Substrate kit (1705060, Bio-Rad, Life Sciences Research) and visualized using the ChemiDoc MP System (1708280, Bio-Rad, Life Sciences Research). Protein levels were analyzed densitometrically using an image analysis system (Image J; National Institute of Health), normalized against values obtained from β-actin blots, and expressed as relative values compared to the vehicle-treated group.

2.8. Planar surface immunoassay

The mouse apoptosis array kit was used to analyze apoptosis-related proteins. From the injured cortical tissues of the vehicle and high dose of TAK-063 (3 mg/kg) were collected, processed through homogenization and sonication, and then treated with a protease/phosphatase inhibitor cocktail (5872, Cell Signaling Technology, USA). We assessed the expression profiles of 21 apoptosis-related proteins, including Catalase, Heme Oxygenase 1 (HO-1/HMOX1/HSP32), myeloid cell leukemia-1 (MCL-1), second mitochondria-derived activator of caspases (SMAC/Diablo), X-linked inhibitor of apoptosis protein (XIAP), Fas receptor (Fas/TNFRSF6/CD95), Hypoxia-inducible factor-1 alpha (HIF-1α), Heat Shock 70 kDa Protein (HSP70/HSPA1A), Tumor protein P53 (p53), Tumor Necrosis Factor Receptor I (TNF RI/TNFRSF1A), BCL2 associated agonist of cell death (Bad), B-cell lymphoma-2 (Bcl-2), Cleaved Caspase-3, Claspin, Heat Shock 60 kDa Protein (HSP60), Bcl-x, Cytochrome c, Heme oxygenase-2 (HO-2/HMOX2), cyclin-dependent kinase inhibitor p27 (p27/Kip1), Tumor necrosis factor receptor superfamily member 10B (TNFRSF10B). This analysis was conducted using the Proteome Profiler Mouse Apoptosis Array Kit (ARY031, R&D Systems, USA) with samples obtained from a total of 9 animals (comprising 3 in the vehicle group, 3 in the 0.3 mg/kg TAK-063 group, and 3 in the 3 mg/kg TAK-063 group), following the manufacturer's instructions. We visualized the array panels using the ChemiDoc MP System (1708280, Biorad Life Sciences Research, USA) and quantified protein levels densitometrically using an image analysis system (Image J). These values were then adjusted based on positive controls and expressed as relative values compared to the treated group.

2.9. Statistical analysis

Statistical analyses were conducted using SPSS (version 15, SPSS Inc., USA) software. Data were evaluated by one-way ANOVA followed

by LSD tests (for PDE10A Western blot, infarct volume, brain swelling, neuronal injury, and DNA fragmentation) or independent samples *t*-test (for mouse apoptosis array and Western blot experiments). Data are presented as mean ± S.D. values. Throughout the study, p values < 0.05 were considered statistically significant.

3. Results

3.1. PDE10A inhibition reduces brain injury and swelling and improves BBB integrity after TBI

It is a well-known fact that PDE10A is a dual cAMP/cGMP hydrolyzing enzyme highly distributed in the striatum and cortex (Heckman et al., 2016; Kelly et al., 2014). Post-traumatic cerebral infarction and brain edema are the most severe insults after TBI. A single oral administration of a low dose (0.3 mg/kg) of TAK-063 did not significantly reduce the infarct volume (Fig. 1A). However, the administration of a high dose (3 mg/kg) of TAK-063 significantly decreased the infarcted area after TBI. Notably, both doses of TAK-063 reduced brain swelling dose-dependently (Fig. 1B). To evaluate BBB disruption, we performed Evans blue staining (Fig. 1C), and the results demonstrated that the low dose did not improve BBB integrity, but the high dose significantly improved BBB integrity after TBI (Fig. 1D).

3.2. PDE10A inhibition increases neuronal survival and decreases apoptotic cell death

To assess neuronal survival, we utilized NeuN staining of coronal sections (Fig. 2A). The number of NeuN-positive cells was quantified from six different regions of interest within both the cortex of the ipsilesional and contralesional hemispheres. Remarkably, both low and high doses of TAK-063 significantly improved neuronal survival (Fig. 2A). In our investigation of widespread neuronal injury in the cerebral cortex, we conducted a terminal deoxynucleotidyl transferase dUTP nick end labeling (TUNEL) assay (Fig. 2B). While the low dose of TAK-063 resulted in a slight reduction in the number of DNA fragmented cells, this reduction was not statistically significant. However, it's noteworthy that the high dose of TAK-063 significantly reduced the number of apoptotic cells after TBI (Fig. 2B). To assess neuronal apoptosis, double staining with TUNEL and NeuN was performed, and the number of double-stained cells in the injured cortex was counted. The results demonstrated that the administration of TAK-063 at doses of 0.3 mg/kg and 3 mg/kg significantly reduced the number of TUNEL-positive neurons compared to the vehicle-treated group (Fig. 2C).

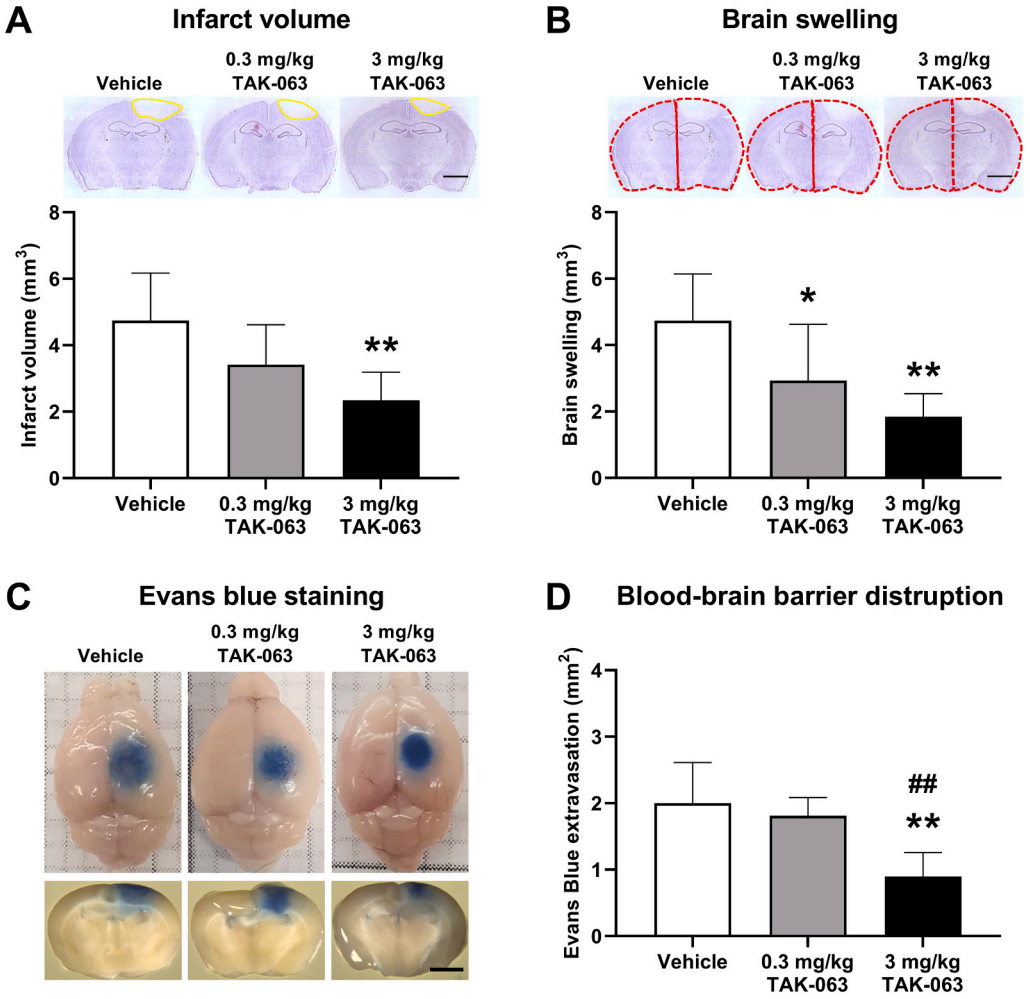

Fig. 1. TAK-063 reduced infarct volume, brain swelling, and BBB disruption after TBI. To evaluate brain infarct volume (A) and brain swelling (B) cresyl violet staining was performed. Yellow lines indicate the area of brain infarction and red lines indicate the whole brain area. Notably, TAK-063 decreased brain infarct volume and brain swelling in a dose-dependent manner. BBB leakage was determined by perfusing mice with Evans blue dye, which is a widely used tracer to assess BBB integrity (C). Notably, a high dose of TAK-063 (3 mg/kg) significantly improved BBB integrity compared to both the vehicle and the low-dose TAK-063 group (D). Data are represented as mean + S.D. ($n = 7$ mice* 3 images for A and B, $n = 4$ mice* 2 images for C and D). $^{**}p < 0.01/^{*}p < 0.05$ compared with vehicle-treated group, $^{\#\#}p < 0.01$ compared with low dose (0.3 mg/kg) TAK-063 treated group. Scale bars 1 mm.

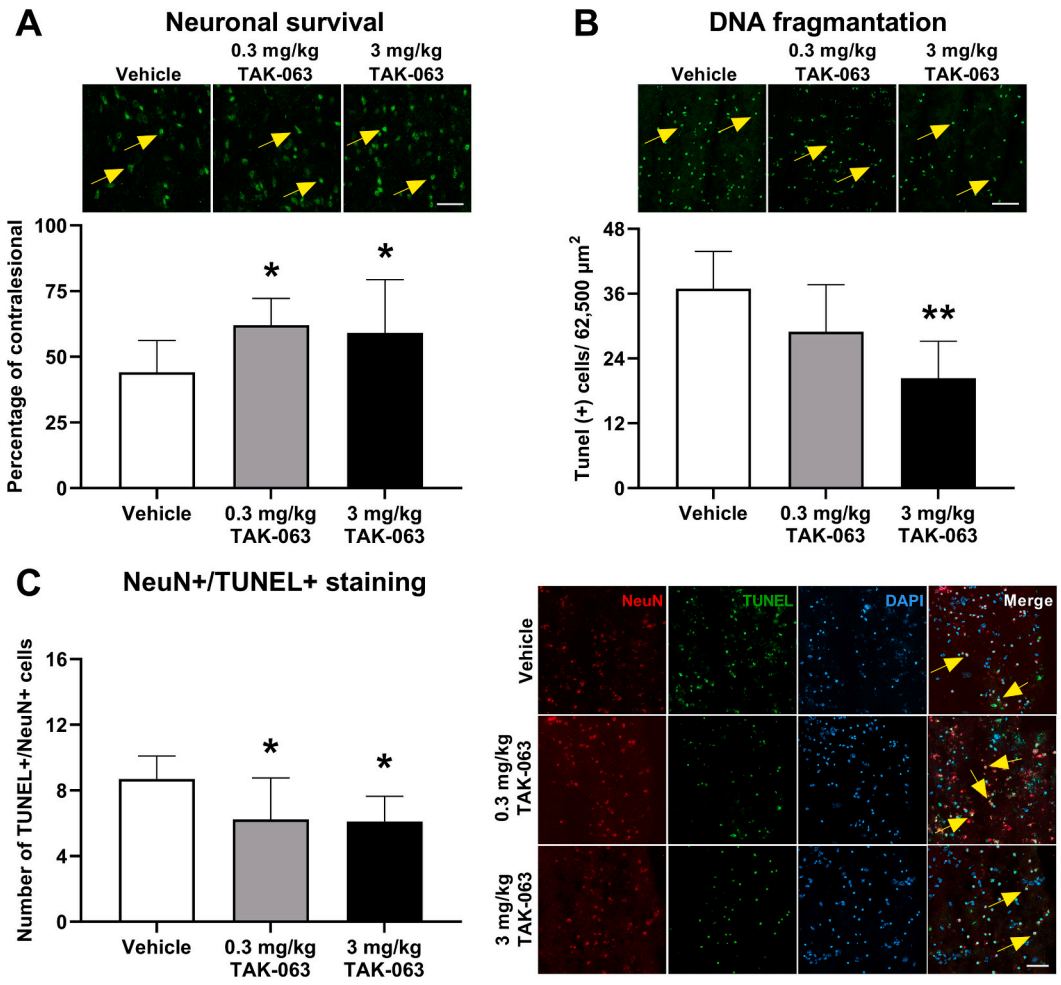

Fig. 2. PDE10A inhibition increases neuronal survival and decreases DNA fragmentation and neuronal apoptosis in the injured tissue. Both low and high doses of TAK-063 increased neuronal survival, which was analyzed by NeuN staining after TBI (A). In addition, a high but not low dose of TAK-063 reduced disseminated neuronal injury, which was evaluated by the terminal deoxynucleotidyl transferase dUTP nick end labeling (TUNEL) assay kit (B). Notably, both doses of TAK-063 reduced neuronal apoptosis in the injured cortex (C). Yellow arrows indicate NeuN-positive cells in A, TUNEL+ cells in B, and NeuN + TUNEL positive cells in C. Data are represented as mean + S.D. ($n = 7$ mice* 2 images for A, B, and C). $^{**}p < 0.01$/$^{*}p < 0.05$ compared with vehicle treated group. Scale bars 100 µm.

3.3. A high dose of TAK-063 increases cAMP levels and decreases PDE10A abundance, thereby mediating the phosphorylation of survival kinases AKT and ERK-1/-2 and inhibiting the abundance of p-PTEN, MMP9, iNOS, and nNOS proteins

Compared to the administration of 0.3 mg/kg TAK-063, the 3 mg/kg dose significantly reduced apoptotic cell death. Therefore, animals treated with 3 mg/kg TAK-063 were selected for the analysis of cell survival and apoptosis-related proteins. First, we assessed cAMP concentrations in the ipsilateral cortex using an enzyme-linked immunosorbent assay (ELISA). Results indicated that the higher dose of TAK-063 led to a notable increase in cAMP levels in the ipsilateral tissue compared to the vehicle-treated group (Fig. 3A). As expected, the high dose of TAK-063 also significantly decreased PDE10A protein abundance (Fig. 3B). PDE10A inhibition increased phosphorylated AKT protein levels, regulating signaling processes such as cell survival, metabolism, and proliferation (Fig. 3C). Here, we observed that PDE10A inhibition decreases PTEN activation, which remains the primary negative regulator of the phosphatidylinositol 3-kinase (PI3K)/AKT signaling pathway (Fig. 3D). Additionally, enhanced ERK-1/-2 activation was observed in the TAK-063 group, playing a central role in cell survival and proliferation (Fig. 3E). Our findings also indicate that TAK-063 decreased pro-inflammatory Matrix metalloproteinase-9 (MMP9) expression, thus preventing BBB disruption after brain injury (Fig. 3F). Moreover, we analyzed the inducible nitric oxide synthase (iNOS) and neuronal nitric oxide synthase (nNOS), which increase nitric oxide (NO) production and trigger neuroinflammation and apoptosis after acute tissue degeneration. Our data reveals that high dose of TAK-063 significantly decreased iNOS and nNOS (Fig. 3G, H).

3.4. PDE10A regulates apoptosis-related proteins

Using a planar surface immunoassay, we conducted a detailed analysis of apoptosis signaling to evaluate the impact of PDE10A inhibition (Fig. 4A–B). The results are shown as a heat map in Fig. 4C using the online platform (https://www.bioinformatics.com.cn) (Tang et al., 2023). PDE10A inhibition decreased the expression of pro-apoptotic TNFRSF1A, TNFRSF10B, and TNFRSF6 receptors. Furthermore, we observed that PDE10A inhibition reduced the levels of pro-apoptotic proteins, including Bad, Bcl-2, cleaved Caspase-3, Cytochrome-c, p27, and p53. Interestingly, TAK-063 significantly reduced the levels of anti-apoptotic proteins or enzymes, including Catalase, Claspin, HIF1α, and XIAP. Notably, PDE10A inhibition did not affect the expression or activation of Bcl-x, HO-1, HO-2, HSP27, HSP60, HSP70, MCL-1, and SMAC. Taken together, these observations suggest that TAK-063 regulates cellular signaling predominantly pro-apoptotic pathways (Fig. 5).

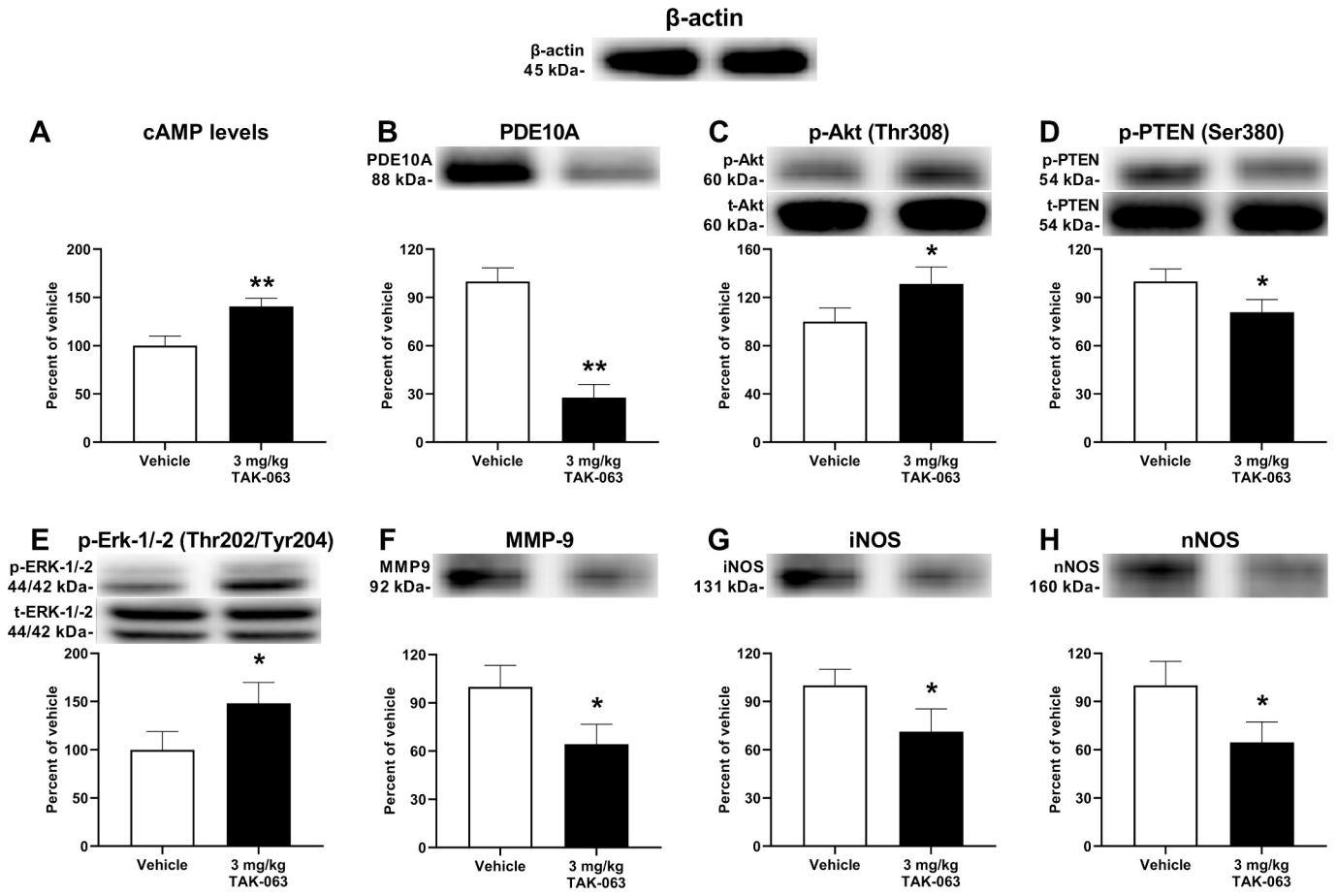

Fig. 3. A high dose of TAK-063 activates pro-survival p-AKT and p-ERK and inhibits p-PTEN, MMP9, iNOS, and nNOS abundance after TBI. ELISA analysis for cAMP (A) and Western blotting for PDE10A (B), p-AKT/AKT (C), p-PTEN/PTEN (D), p-ERK-1/-2/ERK-1/-2 (E), MMP-9 (F), iNOS (G), and nNOS (H). A high dose of TAK-063 significantly reduced PDE10A protein abundance, increased pro-survival AKT, and decreased p-PTEN, the primary negative regulator of the PI3K-Akt signal transduction pathway. In addition, a high dose of TAK-063 increases pro-survival ERK-1/-2 protein expression and decreases MMP9 protein expression, which is important for BBB leakage. Moreover, the inhibition of PDE10A significantly decreased iNOS and nNOS protein expression. Representative images of Western blot analysis from three independent experiments were given above their corresponding graphs. Data are represented as mean ± S.D. values of three independent experiments. $*p < 0.05$ compared with the vehicle-treated group.

4. Discussion

PDEs are dual-specific enzymes that regulate cAMP and cGMP signal transduction pathways. These second messengers modulate diverse signaling pathways through direct interactions with PKA and PKG, including cell survival after neurodegenerative disorders (Li et al., 2024). Among the 11 identified PDEs, PDE10A has emerged as a significant target in the treatment of neurodegenerative disorders (Ahmad et al., 2014; Birjandi et al., 2021; Cardinale and Fusco, 2018). Consequently, the current study demonstrated that TAK-063-mediated PDE10A inhibition reduces brain injury, brain swelling, and disseminated neuronal injury and improves BBB integrity and neuronal survival after TBI in mice. We have also demonstrated that PDE10A inhibition increases the phosphorylation of survival kinases Akt and Erk-1/2 and decreases pro-inflammatory or pro-apoptotic p-PTEN, MMP-9, iNOS, and nNOS analyzed by Western blot. More profoundly, using a planar surface immunoassay, we further analyzed apoptosis signaling and observed that PDE10A inhibition regulates apoptosis. Decreased expression of pro-apoptotic TNFRSF1A, TRAIL-R2, and TNFRSF6 receptors and p27, Cytochrome-c, cleaved Caspase-3, Bad, Bcl-2 and p53 were observed TAK-063 after TBI. Interestingly, PDE10A inhibition also reduced anti-apoptotic known proteins such as XIAP, Catalase, Claspin, and HIF1α. However, compared with the vehicle, PDE10A inhibition did not affect Bcl-x, MCL-1, SMAC, HO-1, HO-2, HSP27, HSP60, and HSP70 proteins.

TBI causes significant mortality, morbidity, and disability worldwide. Annually, >50 million new cases of TBI occur (Collaborators, 2019). TBI can have immediate and enduring impacts on an individual's health, encompassing physical, emotional, and psychosocial changes. TBI is characterized by two distinct phases: primary injury, resulting from mechanical damage during the initial impact, and secondary brain damage, which arises from delayed neurochemical processes and intracellular signaling pathways. These combined effects contribute to the complex and multifaceted nature of TBI's consequences. TBI causes rapid energy depletion, disrupting cell membrane potential and neuronal depolarization (Akamatsu and Hanafy, 2020; Ren and Lu, 2019). Therefore, it induces cell death predominantly in the cerebral cortex, brain swelling, and BBB leakage.

A well-known inhibitor of PDE10A is TAK-063, which is potent, selective, and orally activated (Harada et al., 2015; Suzuki et al., 2015). It can easily cross the BBB and increase the cAMP and cGMP concentration (Tohyama et al., 2018). It was demonstrated that PDE10A occupancy increases in the rat striatum in a dose-dependent manner following oral administration of TAK-063, using non-radiolabeled T-773 as a tracer (Harada et al., 2015). Additionally, oral doses of TAK-063 up to 3 mg/kg did not affect plasma prolactin and glucose levels in rats (Suzuki and Kimura, 2018). In addition, studies in the literature have used TAK-063 at doses ranging from 0.3 to 3 mg/kg for PDE10A inhibition in

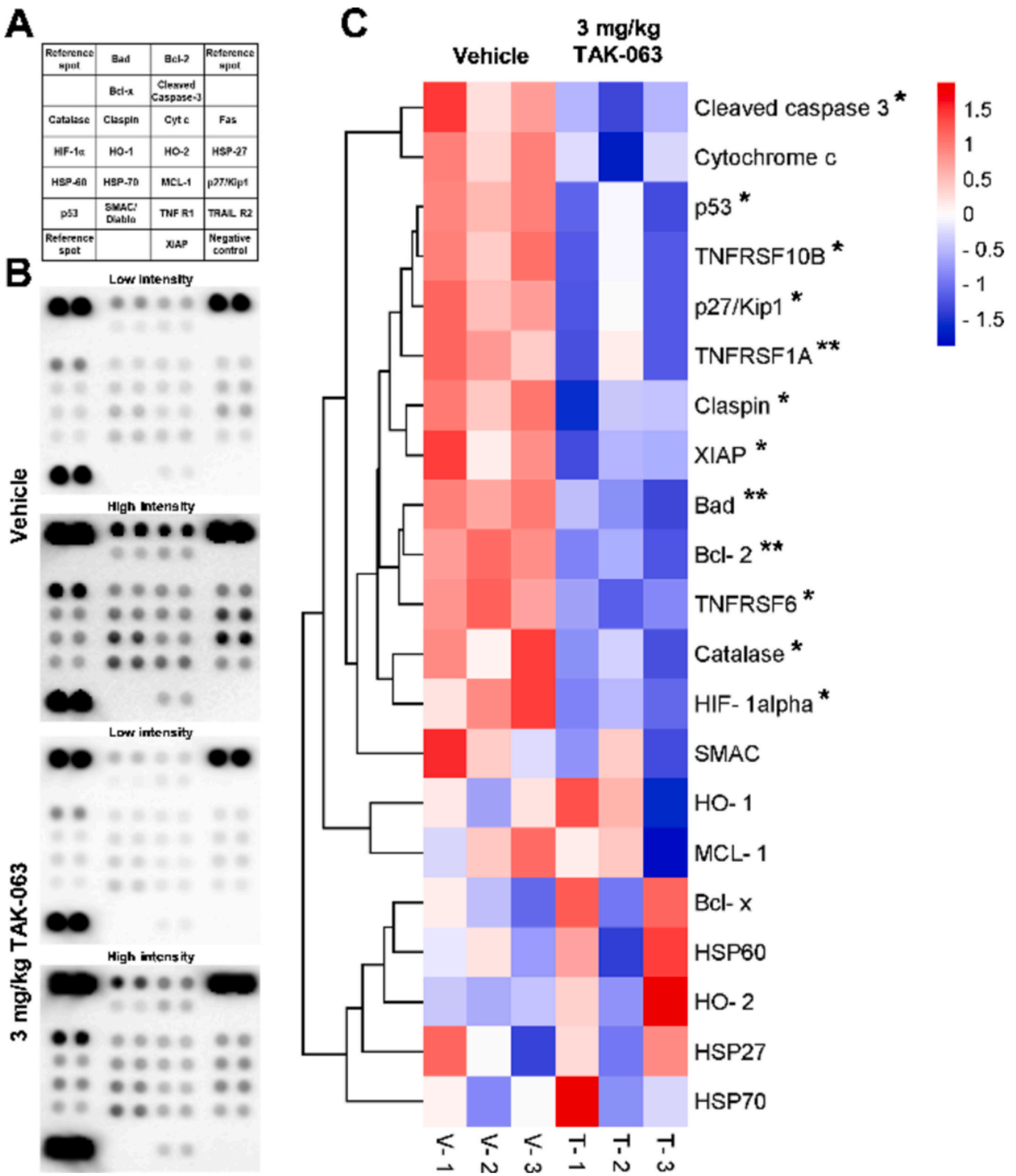

Fig. 4. High dose of TAK-063 decreases pro-apoptotic Bad, Bcl-2, cleaved caspase-3, TNFRSF6, HIF-1α, p27, p53, TNF, TNFRSF10B, and XIAP protein expression in the injured cortex. A map of the apoptotic proteins detected by the antibody array (A). Representative images for mouse apoptosis signaling array (B). Protein analysis for TNFRSF1A, TNFRSF10B, TNFRSF6, Bad, Bcl-2, cleaved Caspase-3, Cytochrome-c, p27, p53, Catalase, Claspin, HIF1α, XIAP, Bcl-x, HO-1, HO-2, HSP27, HSP60, HSP70, MCL-1, and SMAC in the ipsilesional tissue. Inhibition of PDE10A significantly decreased apoptotic Bad, cleaved caspase-3, cytochrome *c*, SMAC, TNFRSF6, p27, TNF R1, and TNFRSF10B protein expression. However, PDE10A inhibition slightly but not significantly reduced the anti-apoptotic Bcl-2 and Bcl-x protein expression. Noted that PDE10A inhibition also decreased the p53 and HIF-1α protein expression, a master regulator of hypoxia/ischemia. The data shows the result of three independent experimental replicates as a heat map. $^{**}p < 0.01/^{*}p < 0.05$ compared with vehicle treated group.

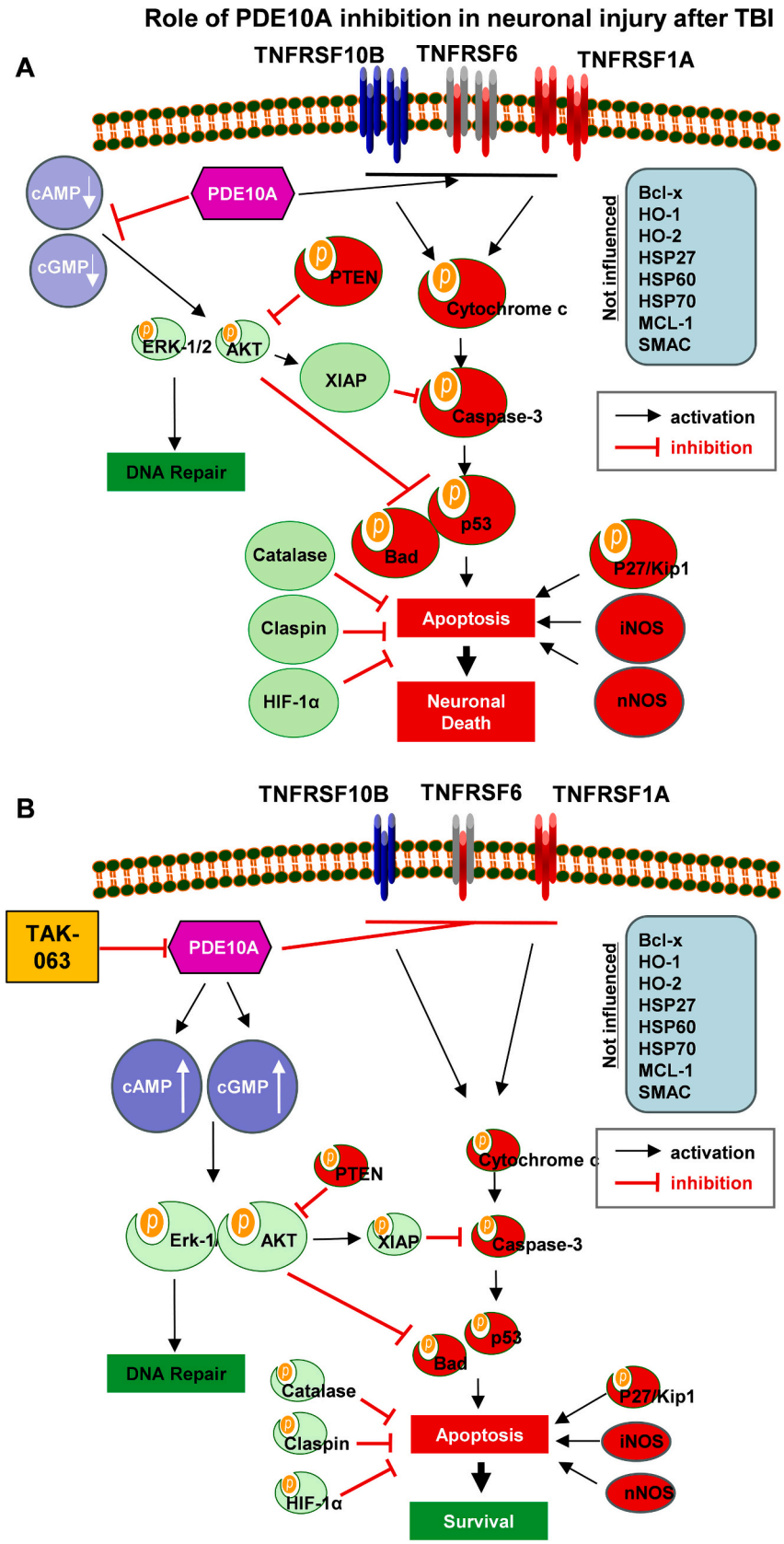

(caption on next page)

Fig. 5. Scheme outlining the role of PDE10A inhibition by TAK-063 in regulating neuronal survival in the injured brain after TBI. When PDE10A is active in A) and inhibited by TAK-063 in B), phosphorylation of survival kinases AKT and ERK-1/2 are increased in TAK-063, which is associated with the increased activation of MMP-9 and PTEN. Furthermore, pro-apoptotic iNOS and nNOS levels are decreased in TAK-063. We observed that inhibition of PDE10A resulted in reduced expression of TNFRSF1A, TNFRSF10B, and TNFRSF6 receptors, inducing particularly apoptotic cell death. These results were also associated with reduced pro-apoptotic proteins, such as PTEN, p27, Cytochrome-c, cleaved Caspase-3, Bad, and p53. Interestingly, TAK-063 treatment reduced anti-apoptotic proteins or enzymes, XIAP, Claspin, and HIF1α. Bcl-x, MCL-1, SMAC, HO-1, HO-2, HSP27, HSP60, and HSP70 were not affected by TAK-063.

laboratory animals (Beker et al., 2022a; Beker et al., 2022b). Therefore, 0.3 mg/kg (low dose) and 3 mg/kg (high dose) TAK-063 were preferred for PDE10A inhibition in the current study.

TAK-063 has been studied for potential therapeutic applications in various neurological and psychiatric disorders due to its effects on critical intracellular signal transduction pathways. A recent study demonstrated that TAK-063 enhanced motor recovery following striatal ischemic injury in a dose-dependent manner, correlated with increased axonal neuroplasticity in the motor system and increased BDNF expression (Birjandi et al., 2021). Furthermore, our recent study revealed that the pharmacological inhibition of PDE10A activates the PI3K/Akt intracellular signaling pathway and upregulates pro- and anti-inflammatory cytokines/chemokines after transient focal ischemia. We also demonstrated that these effects attenuate brain damage in a mouse model of cerebral ischemia. (Beker et al., 2022a). In the current study, the increase in brain damage volume following TBI likely reflects a combination of primary mechanical injury and secondary injury processes such as excitotoxicity, oxidative stress, and inflammation. However, treatment with TAK-063 significantly mitigated these effects by reducing brain damage volume, thereby indicating its potential to counteract these secondary injury processes. The observed brain edema, which typically exacerbates damage by increasing intracranial pressure and leading to further neuronal death and functional impairments, was also significantly reduced by TAK-063 in a dose-dependently manner. Additionally, TAK-063 treatment helped maintain BBB permeability, suggesting that the high dose of TAK-063 effectively preserves the integrity of the tightly regulated barrier. This preservation likely prevents the infiltration of harmful substances into the brain parenchyma, thereby reducing the risk of exacerbating neuroinflammation and tissue damage.

We also assessed the effects of PDE10A inhibition on neuronal survival and DNA fragmentation. Following TBI, TAK-063-increased cAMP and cGMP levels, which in turn enhanced neuronal survival. It is widely recognized that cAMP and cGMP signaling play critical roles in neuronal survival, metabolism, and axonal growth (Boczek et al., 2019). One possible mechanism by which TAK-063-induced cAMP and cGMP levels could promote neuronal survival is through the activation of the PI3K/AKT signal transduction pathway. Notably, while a low dose of TAK-063 did not significantly reduce the number of apoptotic cells in the ipsilesional cortex, a high dose of TAK-063 did decrease the number of DNA-fragmented cells in this region. Importantly, both doses of TAK-063 significantly decreased the overall number of apoptotic neurons in the ipsilesional cortex.

To explore the mechanism responsible for TAK-063-induced recovery following TBI, we conducted a Western blot analysis to examine signal transduction pathways associated with neuronal survival and BBB integrity. PDE10A inhibition has been reported to promote dopamine-mediated cAMP/PKA, PI3K/AKT, ERK, and nNOS/cGMP/PKG signaling (Hsu et al., 2011; Padovan-Neto et al., 2015; Polito et al., 2015). Our findings demonstrated that PDE10A inhibition decreased the phosphorylation of PTEN, a key negative regulator of the PI3K/Akt signaling pathway, which controls critical cellular functions such as survival, proliferation, and metabolism (Kilic et al., 2017; Shi et al., 2019). Additionally, PDE10A inhibition increased the levels of phosphorylated Akt and ERK proteins. This increase is likely due to elevated cAMP and cGMP levels following PDE10A inhibition, which activate downstream signaling molecules like PKA and PKG-both upstream regulators of the PI3K/AKT and MEK/ERK pathways. These pathways, in turn, promote AKT and ERK phosphorylation, enhancing cell survival and reducing apoptosis. Although PDE10A does not directly phosphorylate AKT or ERK, its inhibition triggers a cascade of signaling events via cAMP and cGMP, leading to the observed increase in AKT and ERK phosphorylation. These findings are consistent with previous studies suggesting that the neuroprotective effects of PDE10A inhibition are mediated through enhanced survival signaling pathways. Future studies should investigate the molecular intermediates involved, with a particular focus on inhibiting the PI3K/Akt and MEK/ERK pathways using selective inhibitors. This would help clarify the precise role of PDE10A in modulating these pathways and its contribution to neuronal survival.

TBI leads to BBB disruption, the protective and selective barrier between the brain and the intravascular compartment (Nian et al., 2020). To support the effects of TAK-063 on BBB leakage, which was assessed by Evans blue staining, we analyzed MMP9 protein expression by Western blotting. We showed that PDE10A inhibition decreased the MMP9 protein expression, which prevented BBB disruption after brain injury. Furthermore, we analyzed the iNOS and nNOS protein expression, which can contribute to neuroprotection and neurotoxicity, depending on factors such as the type and severity of injury. Studies reported that iNOS-derived NO production exacerbated brain injury and BBB integrity after neuronal injury, such as TBI and stroke (Parathath et al., 2007; Wang and Han, 2018). A notable finding is that PDE10A inhibition decreased iNOS and nNOS protein abundance, and it is suggested that the severity of neuronal injury was reduced.

To analyze the effects of PDE10A inhibition on apoptosis, we performed a planar surface immunoassay of ipsilesional cortical brain tissue. For this, we chose a high dose of TAK-063, which increased neuronal survival and reduced DNA fragmentation more effectively than a low dose. PDE10A inhibition reduced the expression of cytochrome *c*- and SMAC, a mitochondrial protein that triggers cytochrome *c* release and disrupts the mitochondrial membrane potential during apoptosis. Therefore, the cleaved caspase-3 protein expression level was reduced by TAK-063 administration. BCL-2 family proteins (BAD, BCL-2, and BCL-xL) are important programmed cell death pathway regulators. PDE10A inhibition reduced the pro-apoptotic BAD protein level. Interestingly, PDE10A inhibition slightly but not significantly decreased anti-apoptotic Bcl-x and Bcl-2 protein expression. Further analysis showed that PDE10A inhibition also reduced the protein expression of TNFR2 and TNFRSF10B, which are involved in both apoptosis and immune system regulation. These receptors play a crucial role in modulating immune responses, particularly in inflammation and the activation of Nuclear Factor kappa B (NF-κB), which is key to immune cell survival and function (Capece et al., 2022). Compelling evidence indicates that TAK-063 led to a reduction in the level of HIF-1α, a master regulator of hypoxia/ischemia, which is essential in neuronal repair mechanisms, inflammation, apoptosis, BBB integrity, and the immune system's adaptation after brain injury (Khan et al., 2017; Yang et al., 2017). According to our data, the inhibition of PDE10A by TAK-063 reduced HIF-1α protein expression. Moreover, inhibition of PDE10A also reduced the level of the tumor suppressor p53, which plays an essential role in DNA repair and apoptosis. These findings suggest that the proteins analyzed in our study not only play a role in the cellular response to injury but also significantly contribute to the regulation and execution of immune responses during TBI.

Considering the results obtained in this study, TAK-063-mediated PDE10A inhibition emerges as a promising strategy for reducing brain injury, swelling disseminated neuronal injury, and promoting increased

neuronal survival after TBI in mice. Moreover, our findings highlight that PDE10A inhibition is associated with decreased pro-apoptotic protein expressions and increased survival kinases AKT and ERK-1/-2. The current results also indicate that PDE10A inhibition regulates apoptosis signaling and profoundly stimulates anti-apoptotic proteins. However, further studies are necessary to elucidate the direct or indirect effects of PDE10A inhibition on cell death or apoptosis signaling.

Ethical approval

This study has been conducted under the ethics standards of the EU Guidelines on the Care and Use of Laboratory Animals (Directive 2010/63/EU) in agreement with local guidelines and legislation. The study has been approved by local government authorities (Istanbul Medipol University, Animal Research Ethics Committee; reference number: 03/02/2021-10).

Funding

This work was supported by the Turkish Academy of Sciences (TUBA; to EK).

CRediT authorship contribution statement

Mustafa C. Beker: Writing – review & editing, Writing – original draft, Software, Project administration, Methodology, Investigation. **Mehmet O. Altintas:** Investigation. **Enes Dogan:** Methodology, Investigation. **Cigdem Bayraktaroglu:** Methodology, Investigation. **Buse Balaban:** Software, Investigation. **Aysenur Ozpinar:** Methodology, Investigation. **Nursena Sengun:** Software, Methodology, Investigation. **Serdar Altunay:** Writing – original draft, Supervision, Software. **Ertugrul Kilic:** Writing – review & editing, Writing – original draft, Supervision, Funding acquisition.

Declaration of competing interest

The authors declare the following financial interests/personal relationships which may be considered as potential competing interests: Ertugrul Kilic reports financial support was provided by Turkish Academy of Sciences. If there are other authors, they declare that they have no known competing financial interests or personal relationships that could have appeared to influence the work reported in this paper.

Acknowledgments

This work was supported by Turkish Academy of Sciences (TUBA; EK).

We thank Melih A. Yıldırım for his contribution to animal care.

Data availability

The raw data from this study are available from the corresponding authors upon reasonable request.

References

Ahmad, R., Bourgeois, S., Postnov, A., Schmidt, M.E., Bormans, G., Van Laere, K., Vandenberghe, W., 2014. PET imaging shows loss of striatal PDE10A in patients with Huntington disease. Neurology 82, 279–281.

Akamatsu, Y., Hanafy, K.A., 2020. Cell death and recovery in traumatic brain injury. Neurotherapeutics: the journal of the American Society for Experimental NeuroTherapeutics 17, 446–456.

Argyrousi, E.K., Heckman, P.R.A., Prickaerts, J., 2020. Role of cyclic nucleotides and their downstream signaling cascades in memory function: being at the right time at the right spot. Neurosci. Biobehav. Rev. 113, 12–38.

Beker, M.C., Caglayan, A.B., Kelestemur, T., Caglayan, B., Yalcin, E., Yulug, B., Kilic, U., Hermann, D.M., Kilic, E., 2015. Effects of normobaric oxygen and melatonin on reperfusion injury: role of cerebral microcirculation. Oncotarget 6, 30604–30614.

Beker, M.C., Caglayan, B., Caglayan, A.B., Kelestemur, T., Yalcin, E., Caglayan, A., Kilic, U., Baykal, A.T., Reiter, R.J., Kilic, E., 2019. Interaction of melatonin and Bmal1 in the regulation of PI3K/AKT pathway components and cellular survival. Sci. Rep. 9, 19082.

Beker, M., Caglayan, A.B., Beker, M.C., Altunay, S., Karacay, R., Dalay, A., Altintas, M.O., Kose, G.T., Hermann, D.M., Kilic, E., 2020. Lentivirally administered glial cell line-derived neurotrophic factor promotes post-ischemic neurological recovery, brain remodeling and contralesional pyramidal tract plasticity by regulating axonal growth inhibitors and guidance proteins. Exp. Neurol. 331, 113364.

Beker, M.C., Caglayan, A.B., Altunay, S., Ozbay, E., Ates, N., Kelestemur, T., Caglayan, B., Kilic, U., Doeppner, T.R., Hermann, D.M., Kilic, E., 2022a. Phosphodiesterase 10A is a critical target for neuroprotection in a mouse model of ischemic stroke. Mol. Neurobiol. 59, 574–589.

Beker, M.C., Pence, M.E., Yagmur, S., Caglayan, B., Caglayan, A., Kilic, U., Yelkenci, H.E., Altintas, M.O., Caglayan, A.B., Doeppner, T.R., Hermann, D.M., Kilic, E., 2022b. Phosphodiesterase 10A deactivation induces long-term neurological recovery, Peri-infarct remodeling and pyramidal tract plasticity after transient focal cerebral ischemia in mice. Exp. Neurol. 358, 114221.

Birjandi, S.Z., Abduljawad, N., Nair, S., Dehghani, M., Suzuki, K., Kimura, H., Carmichael, S.T., 2021. Phosphodiesterase 10A inhibition leads to brain region-specific recovery based on stroke type. Transl. Stroke Res. 12, 303–315.

Boczek, T., Cameron, E.G., Yu, W., Xia, X., Shah, S.H., Castillo Chabeco, B., Galvao, J., Nahmou, M., Li, J., Thakur, H., Goldberg, J.L., Kapiloff, M.S., 2019. Regulation of neuronal survival and axon growth by a perinuclear cAMP compartment. J. Neurosci. 39, 5466–5480.

Capece, D., Verzella, D., Flati, I., Arboretto, P., Cornice, J., Franzoso, G., 2022. NF-kappaB: blending metabolism, immunity, and inflammation. Trends Immunol. 43, 757–775.

Cardinale, A., Fusco, F.R., 2018. Inhibition of phosphodiesterases as a strategy to achieve neuroprotection in Huntington's disease. CNS Neurosci. Ther. 24, 319–328.

Ciftci, E., Karacay, R., Caglayan, A., Altunay, S., Ates, N., Altintas, M.O., Doeppner, T.R., Yulug, B., Kilic, E., 2020. Neuroprotective effect of lithium in cold-induced traumatic brain injury in mice. Behav. Brain Res. 392, 112719.

Collaborators, G.B.D.N., 2019. Global, regional, and national burden of neurological disorders, 1990–2016: a systematic analysis for the global burden of disease study 2016. The Lancet. Neurology 18, 459–480.

Delhaye, S., Bardoni, B., 2021. Role of phosphodiesterases in the pathophysiology of neurodevelopmental disorders. Mol. Psychiatry 26, 4570–4582.

Elibol, B., Beker, M., Terzioglu-Usak, S., Dalli, T., Kilic, U., 2020. Thymoquinone administration ameliorates Alzheimer's disease-like phenotype by promoting cell survival in the hippocampus of amyloid beta(1-42) infused rat model. Phytomedicine 79, 153324.

Garcia, A.M., Redondo, M., Martinez, A., Gil, C., 2014. Phosphodiesterase 10 inhibitors: new disease modifying drugs for Parkinson's disease? Curr. Med. Chem. 21, 1171–1187.

Giampa, C., Laurenti, D., Anzilotti, S., Bernardi, G., Menniti, F.S., Fusco, F.R., 2010. Inhibition of the striatal specific phosphodiesterase PDE10A ameliorates striatal and cortical pathology in R6/2 mouse model of Huntington's disease. PloS One 5, e13417.

Harada, A., Suzuki, K., Kamiguchi, N., Miyamoto, M., Tohyama, K., Nakashima, K., Taniguchi, T., Kimura, H., 2015. Characterization of binding and inhibitory properties of TAK-063, a novel phosphodiesterase 10A inhibitor. PloS One 10, e0122197.

Heckman, P.R.A., van Duinen, M.A., Bollen, E.P.P., Nishi, A., Wennogle, L.P., Blokland, A., Prickaerts, J., 2016. Phosphodiesterase inhibition and regulation of dopaminergic frontal and striatal functioning: clinical implications. Int. J. Neuropsychopharmacol. 19.

Hermann, D.M., Kilic, E., Kugler, S., Isenmann, S., Bahr, M., 2001. Adenovirus-mediated glial cell line-derived neurotrophic factor (GDNF) expression protects against subsequent cortical cold injury in rats. Neurobiol. Dis. 8, 964–973.

Hsu, Y.T., Liao, G., Bi, X., Oka, T., Tamura, S., Baudry, M., 2011. The PDE10A inhibitor, papaverine, differentially activates ERK in male and female rat striatal slices. Neuropharmacology 61, 1275–1281.

Huang, J., Tang, D., Cao, Y., Wang, Y., Long, J., Wei, L., Song, H., 2022. Inhibition of PDE10A-rescued TBI-induced neuroinflammation and apoptosis through the cAMP/PKA/NLRP3 pathway. Evid. Based Complement. Alternat. Med. 2022, 3311250.

Insel, P.A., Zhang, L., Murray, F., Yokouchi, H., Zambon, A.C., 2012. Cyclic AMP is both a pro-apoptotic and anti-apoptotic second messenger. Acta Physiol (Oxf.) 204, 277–287.

Ito, M., Aswendt, M., Lee, A.G., Ishizaka, S., Cao, Z., Wang, E.H., Levy, S.L., Smerin, D.L., McNab, J.A., Zeineh, M., Leuze, C., Goubran, M., Cheng, M.Y., Steinberg, G.K., 2018. RNA-sequencing analysis revealed a distinct motor cortex transcriptome in spontaneously recovered mice after stroke. Stroke 49, 2191–2199.

Kelestemur, T., Yulug, B., Caglayan, A.B., Beker, M.C., Kilic, U., Caglayan, B., Yalcin, E., Gundogdu, R.Z., Kilic, E., 2016. Targeting different pathophysiological events after traumatic brain injury in mice: role of melatonin and memantine. Neurosci. Lett. 612, 92–97.

Kelly, M.P., Adamowicz, W., Bove, S., Hartman, A.J., Mariga, A., Pathak, G., Reinhart, V., Romegialli, A., Kleiman, R.J., 2014. Select 3′,5′-cyclic nucleotide phosphodiesterases exhibit altered expression in the aged rodent brain. Cell. Signal. 26, 383–397.

Keskin, I., Gunal, M.Y., Ayturk, N., Kilic, U., Ozansoy, M., Kilic, E., 2017. Dose-dependent neuroprotective effect of enoxaparin on cold-induced traumatic brain injury. Neural Regen. Res. 12, 761–764.

Khan, M., Khan, H., Singh, I., Singh, A.K., 2017. Hypoxia inducible factor-1 alpha stabilization for regenerative therapy in traumatic brain injury. Neural Regen. Res. 12, 696–701.

Kilic, U., Caglayan, A.B., Beker, M.C., Gunal, M.Y., Caglayan, B., Yalcin, E., Kelestemur, T., Gundogdu, R.Z., Yulug, B., Yilmaz, B., Kerman, B.E., Kilic, E., 2017. Particular phosphorylation of PI3K/Akt on Thr308 via PDK-1 and PTEN mediates melatonin's neuroprotective activity after focal cerebral ischemia in mice. Redox Biol. 12, 657–665.

Kim, D.Y., Park, J.S., Leem, Y.H., Park, J.E., Kim, H.S., 2021. The potent PDE10A inhibitor MP-10 (PF-2545920) suppresses microglial activation in LPS-induced neuroinflammation and MPTP-induced Parkinson's disease mouse models. J. Neuroimmune Pharmacol. 16, 470–482.

Li, Q., Liao, Q., Qi, S., Huang, H., He, S., Lyu, W., Liang, J., Qin, H., Cheng, Z., Yu, F., Dong, X., Wang, Z., Han, L., Han, Y., 2024. Opportunities and perspectives of small molecular phosphodiesterase inhibitors in neurodegenerative diseases. Eur. J. Med. Chem. 271, 116386.

Lugnier, C., 2022. The complexity and multiplicity of the specific cAMP phosphodiesterase family: PDE4, open new adapted therapeutic approaches. Int. J. Mol. Sci. 23.

Misra, U.K., Pizzo, S.V., 2005. Coordinate regulation of forskolin-induced cellular proliferation in macrophages by protein kinase A/cAMP-response element-binding protein (CREB) and Epac1-Rap1 signaling: effects of silencing CREB gene expression on Akt activation. J. Biol. Chem. 280, 38276–38289.

Nian, K., Harding, I.C., Herman, I.M., Ebong, E.E., 2020. Blood-brain barrier damage in ischemic stroke and its regulation by endothelial mechanotransduction. Front. Physiol. 11, 605398.

Niccolini, F., Haider, S., Reis Marques, T., Muhlert, N., Tziortzi, A.C., Searle, G.E., Natesan, S., Piccini, P., Kapur, S., Rabiner, E.A., Gunn, R.N., Tabrizi, S.J., Politis, M., 2015. Altered PDE10A expression detectable early before symptomatic onset in Huntington's disease. Brain 138, 3016–3029.

Padovan-Neto, F.E., West, A.R., 2017. Regulation of striatal neuron activity by cyclic nucleotide signaling and phosphodiesterase inhibition: implications for the treatment of Parkinson's disease. Adv Neurobiol 17, 257–283.

Padovan-Neto, F.E., Sammut, S., Chakroborty, S., Dec, A.M., Threlfell, S., Campbell, P. W., Mudrakola, V., Harms, J.F., Schmidt, C.J., West, A.R., 2015. Facilitation of corticostriatal transmission following pharmacological inhibition of striatal phosphodiesterase 10A: role of nitric oxide-soluble guanylyl cyclase-cGMP signaling pathways. J. Neurosci. 35, 5781–5791.

Parathath, S.R., Gravanis, I., Tsirka, S.E., 2007. Nitric oxide synthase isoforms undertake unique roles during excitotoxicity. Stroke 38, 1938–1945.

Polito, M., Guiot, E., Gangarossa, G., Longueville, S., Doulazmi, M., Valjent, E., Herve, D., Girault, J.A., Paupardin-Tritsch, D., Castro, L.R., Vincent, P., 2015. Selective effects of PDE10A inhibitors on striatopallidal neurons require phosphatase inhibition by DARPP-32. eNeuro 2.

Ren, H., Lu, H., 2019. Dynamic features of brain edema in rat models of traumatic brain injury. Neuroreport 30, 605–611.

Shi, X., Wang, J., Lei, Y., Cong, C., Tan, D., Zhou, X., 2019. Research progress on the PI3K/AKT signaling pathway in gynecological cancer (review). Mol. Med. Rep. 19, 4529–4535.

Suzuki, K., Kimura, H., 2018. TAK-063, a novel PDE10A inhibitor with balanced activation of direct and indirect pathways, provides a unique opportunity for the treatment of schizophrenia. CNS Neurosci. Ther. 24, 604–614.

Suzuki, K., Harada, A., Shiraishi, E., Kimura, H., 2015. In vivo pharmacological characterization of TAK-063, a potent and selective phosphodiesterase 10A inhibitor with antipsychotic-like activity in rodents. J. Pharmacol. Exp. Ther. 352, 471–479.

Tang, D., Chen, M., Huang, X., Zhang, G., Zeng, L., Zhang, G., Wu, S., Wang, Y., 2023. SRplot: a free online platform for data visualization and graphing. PloS One 18, e0294236.

Titus, D.J., Oliva, A.A., Wilson, N.M., Atkins, C.M., 2015. Phosphodiesterase inhibitors as therapeutics for traumatic brain injury. Curr. Pharm. Des. 21, 332–342.

Tohyama, K., Sudo, M., Morohashi, A., Kato, S., Takahashi, J., Tagawa, Y., 2018. Pre-clinical characterization of absorption, distribution, metabolism and excretion properties of TAK-063. Basic Clin. Pharmacol. Toxicol. 122, 577–587.

Wang, B., Han, S., 2018. Inhibition of inducible nitric oxide synthase attenuates deficits in synaptic plasticity and brain functions following traumatic brain injury. Cerebellum 17, 477–484.

Wilson, N.M., Titus, D.J., Oliva Jr., A.A., Furones, C., Atkins, C.M., 2016. Traumatic brain injury upregulates phosphodiesterase expression in the hippocampus. Front. Syst. Neurosci. 10, 5.

Yang, X.S., Yi, T.L., Zhang, S., Xu, Z.W., Yu, Z.Q., Sun, H.T., Yang, C., Tu, Y., Cheng, S.X., 2017. Hypoxia-inducible factor-1 alpha is involved in RIP-induced necroptosis caused by in vitro and in vivo ischemic brain injury. Sci. Rep. 7, 5818.

Yelkenci, H.E., Degirmenci, Z., Koc, H.I., Bayirli, S., Baltaci, S.B., Altunay, S., Oztekin, N., Kocak, M., Kilic, E., Beker, M.C., 2024. Vinpocetine ameliorates neuronal injury after cold-induced traumatic brain injury in mice. Mol. Neurobiol. 1–17.